

FUSE and the Astrophysics of AGN and QSOs

Gerard A. Kriss

*Space Telescope Science Institute, 3700 San Martin Drive, Baltimore,
 MD 21218, USA*
email: gak@stsci.edu

Abstract. The high spectral resolution and sensitivity of *FUSE* have enabled far-ultraviolet studies of AGN and QSOs that are a natural complement to observations using *HST*, *Chandra*, and *XMM-Newton*. Through synergistic use of the large sample of nearby AGN that serve as background probes of gas in the Galactic halo and the ISM, the *FUSE* PI team has observed a large number (approaching 100) of the nearest and brightest AGN. In addition to emission from O VI, we identify emission lines due to C III, N III, S IV, and He II in many of the Type-1 AGN. More than half of the Type 1 objects also show intrinsic absorption by the O VI doublet as well as C IV absorption and evidence of a soft X-ray warm absorber. Guest investigators have successfully coordinated *FUSE* observations of bright AGN with simultaneous *HST* and X-ray observations. These have contributed greatly to our understanding of the UV and X-ray absorbing gas in AGN as either a wind from the accretion disk, or a thermally driven wind from the obscuring torus.

1. Introduction

Observations of the nearest and brightest active galaxies have inspired our current paradigm for the workings of active galactic nuclei (AGN). Their proximity gives superb spatial scale, which has been exploited in imaging with the *Hubble Space Telescope (HST)* and in high-resolution radio observations. These same nearby AGN have the highest S/N *HST* far-UV spectra, and the best high-resolution X-ray spectra. The spectral energy distribution of AGN peaks in the far-ultraviolet wavelength range. Thus, it is important for understanding the energy generation mechanism and the processes that govern accretion onto massive black holes. Since this portion of the spectrum also determines the radiative input to the broad-line region (BLR) and the narrow-line region (NLR) in AGN, as well as the surrounding host galaxy and the intergalactic medium (IGM), determining its spectral shape is a crucial input for understanding the physical conditions of the gas in surrounding regions. The high spectral resolution and high sensitivity of the *Far Ultraviolet Spectroscopic Explorer (FUSE)* enables us to study the astrophysics of the nearest AGN in this crucial waveband.

The 900–1200 Å spectral range contains numerous diagnostic spectral features that can be applied to AGN physics. The most prominent emission line is the O VI resonance doublet $\lambda\lambda 1032, 1038$, which is particularly strong in the spectra of low-redshift, low-luminosity AGN due to the Baldwin effect (Scott et al. 2004). This line can serve as a diagnostic of the energy input from the extreme ultraviolet to soft X-ray portions of the ionizing continuum.

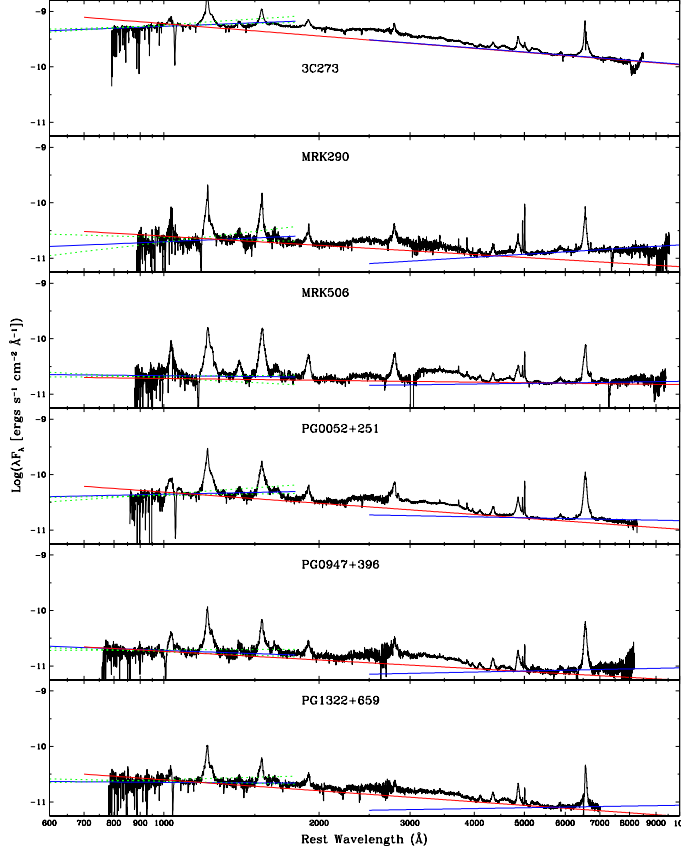


Figure 1. FUV to optical SEDs and fitted power-laws for selected *FUSE* AGN. Dotted lines show the uncertainties in the FUV power-law fits.

Likewise, the O VI doublet is a crucial diagnostic for the absorbing gas commonly seen as O VII and O VIII absorption in X-ray spectra of AGN (Reynolds 1997; George et al. 1998), and as Ly α and C IV absorption in *HST* spectra (Crenshaw et al. 1999). The high-order Lyman lines and the Lyman limit provide additional diagnostics of absorbing gas. In some cases (e.g., NGC 4151 or NGC 3516) the neutral hydrogen can be optically thick and thereby play a significant role in collimating the ionizing radiation that illuminates the NLR (Kriss et al. 1997). Finally, numerous ground-state transitions of molecular hydrogen in the Lyman and Werner bands provide a sensitive tracer of molecular gas. Under the right circumstances, one might expect to see H₂ associated with the obscuring torus in AGN in absorption against the continuum and broad emission lines.

2. The Ionizing Continuum Shape

The ionizing continuum shape in AGN is difficult to study directly. At low redshift it is mostly obscured by our own interstellar medium, and inferences

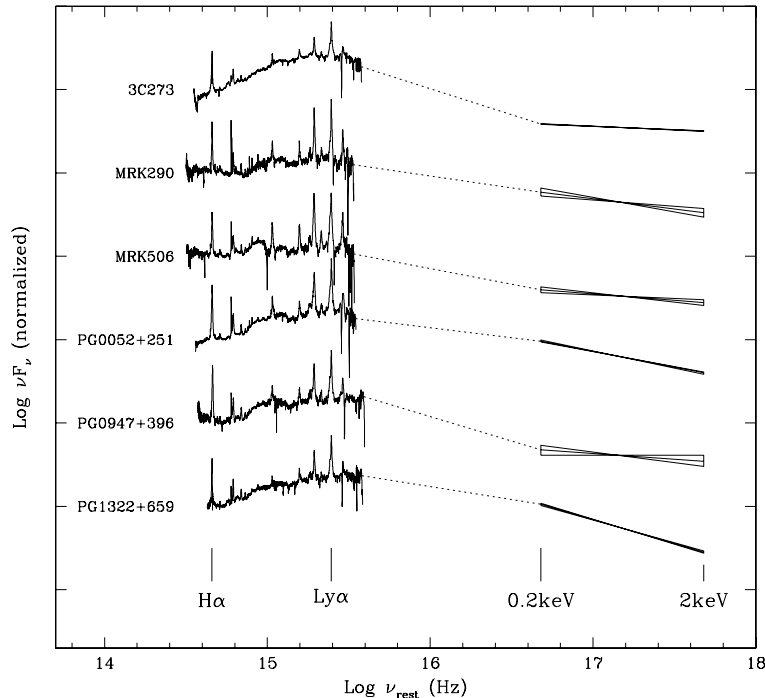


Figure 2. Optical/UV/X-ray spectral energy distributions of representative AGN. The dotted lines are drawn to connect the FUV and X-ray spectra.

must be made from the spectral shape observed in the far-UV and soft X-ray (on either side of the opaque interstellar absorption) as well as from clues provided by the emission lines observed. Composite spectra assembled from *HST* observations of moderate-redshift quasars (Zheng et al. 1997; Telfer et al. 2002) show that the spectral energy distribution of AGN peaks in the far-ultraviolet, with a distinct break at $\sim 1000 \text{ \AA}$. The short wavelength response of *FUSE* allows us to investigate the continuum properties of lower-redshift, lower-luminosity AGN. We have used both the composite spectrum approach, and the detailed assembly of spectral energy distributions for 17 individual AGN.

Shang et al. (2004) obtained quasi-simultaneous observations of 17 AGN using *FUSE*, *HST*, and ground-based telescopes to produce spectral energy distributions covering 912–9000 \AA in the observed frame. A sampling of these spectra in Figure 1 shows that single power laws adequately describe the UV-optical continuum shape of roughly half the sample. Many of the objects, however, show breaks in the spectral index at $\sim 1100 \text{ \AA}$, similar to the *HST* composites. When we compare the UV-optical spectra with archival X-ray spectra (Figure 2), one can see that the spectral energy distribution is clearly peaking in the far-ultraviolet. In most cases, the objects in the Shang et al. (2004) sample have an X-ray spectral slope and normalization matching the extrapolation of the FUV continuum.

These individual SEDs are broadly consistent with modern accretion-disk models. Geometrically thin disk models with non-LTE atmospheres (Hubeny et al.

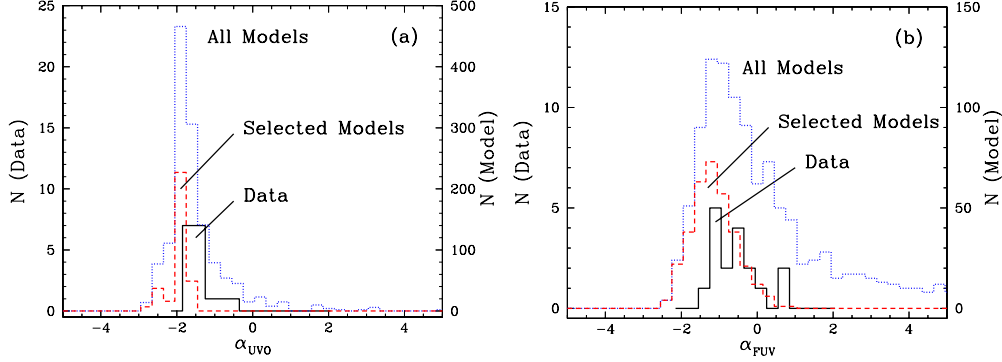


Figure 3. Distributions of α_{uvo} and α_{fuv} for the Shang et al. (2004) sample (solid line), all accretion-disk models (dotted line), and accretion-disk models spanning the same range in mass and Eddington ratio as the sample.

2000) predict a narrow distribution of power-law indices for disk spectra on the red side of the peak in the SED. These models peak in the far-ultraviolet, with a spectral break or bump near the Lyman limit. Spectral indices shortward of the break have a broader distribution. As shown in Figure 3 the 17 AGN from Shang et al. (2004) have roughly similar distributions of spectral indices compared to the models.

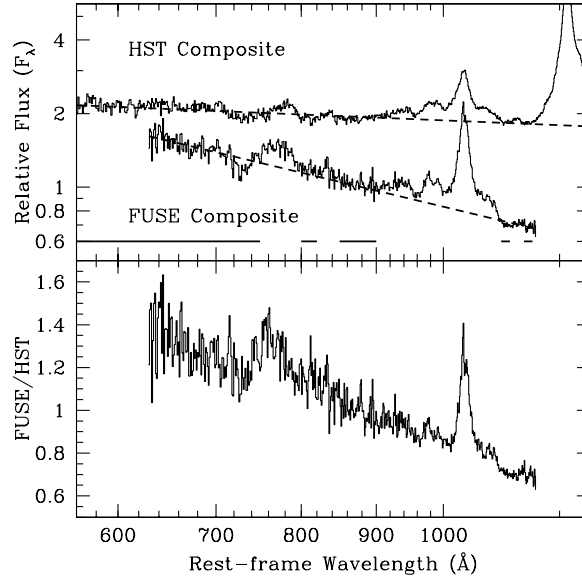


Figure 4. *Top panel:* Composite AGN spectra with power law continuum fits (dashed lines) and wavelength regions used in fit (solid lines). *Bottom panel:* The ratio of the *FUSE* composite to the *HST* composite spectrum.

With the same technique used to create the *HST* composite AGN spectra, we have constructed a composite *FUSE* spectrum from 128 observations of 85 distinct AGN (Scott et al. 2004). As shown in Figure 4, the *FUSE* composite

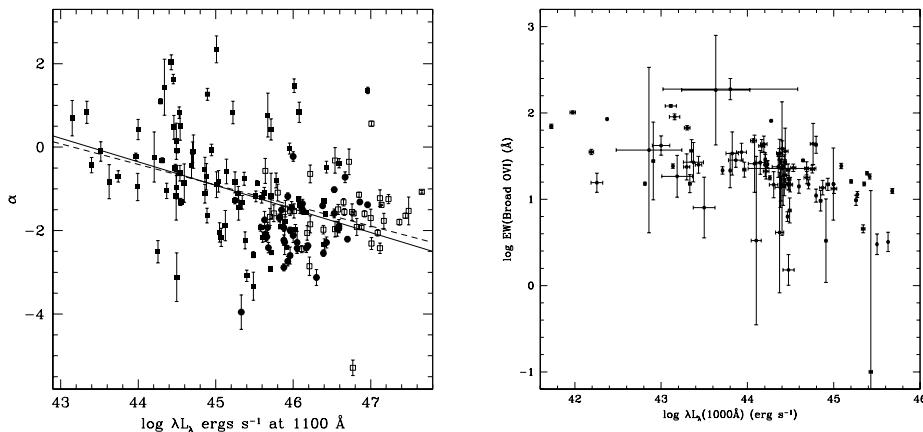


Figure 5. *Left Panel:* EUV spectral index (for $f_\nu \sim \nu^\alpha$) vs. the 1100 Å luminosity for *FUSE* (solid squares) and *HST* (Radio-loud: solid circles, Radio-quiet: open squares) AGN. The dashed line is the best linear fit to the combined *FUSE* and *HST* sample; the solid line is for the *FUSE* sample alone. *Right Panel:* The equivalent width of broad O VI emission in the *FUSE* AGN shows a strong anticorrelation with the continuum luminosity at 1000 Å.

($\alpha = -0.56^{+0.38}_{-0.28}$ for $f_\nu \sim \nu^\alpha$) is bluer than the *HST* composite ($\alpha = -1.76 \pm 0.12$), it shows no evidence for a break in the spectral index in the far-ultraviolet, and it has significantly stronger Ne VIII and O VI emission.

In an effort to understand these properties in more detail, we examined the spectral indices of individual objects in the sample. As found by Shang et al. (2004), some individual objects do show breaks in their spectrum, but, in general, the *FUSE* AGN are lower luminosity and bluer than individual *HST* AGN. The left panel of Figure 5 shows a significant anticorrelation between the AGN spectral index and its luminosity. We interpret this in the context of an accretion disk around the central black hole in the following manner—lower-luminosity AGN are likely to have less massive black holes, and hence hotter accretion disks. This shifts the peak of their spectral energy distributions to shorter wavelengths, moving the spectral break out of the *FUSE* bandpass and making their spectra bluer. This physical interpretation may also explain the Baldwin effect. The bluer spectra will have more high-energy photons, leading to relatively more emission from highly ionized species such as C IV, O VI, and Ne VIII. As shown in the right panel of Figure 5, O VI emission in the *FUSE* sample shows a strong anticorrelation with luminosity.

3. Emission and Absorption Features in *FUSE* AGN Spectra

As of November 1, 2002, *FUSE* spectra for a total of 104 AGN were present in the archive. Four of these are Type 2 AGN, and the rest are Type 1. Two of the Type 2 AGN show strong, narrow emission lines (NGC 1068 and Mrk 477), and the other two have stellar continua typical of starburst galaxies. 53 of the Type 1 AGN have $z < 0.15$, so that the O VI doublet is visible in the *FUSE* band. As

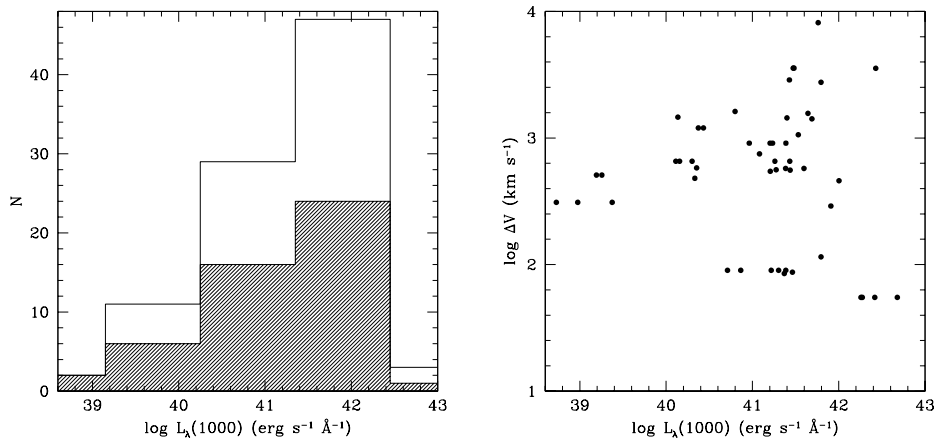


Figure 6. Left: Histogram of *FUSE* AGN versus luminosity. The shaded area shows the number of objects exhibiting intrinsic absorption. Right: The points show outflow velocity as a function of luminosity.

shown earlier in Figure 5, all of these AGN have strong, broad O VI emission. Surprisingly, roughly a third of these (17/53) also show strong *narrow* O VI emission. Emission from C III λ 977 and N III λ 991 is common, as is a bump of blended emission lines on the red wing of O VI. In narrow-line Seyfert 1 galaxies such as I Zw 1, this bump is resolved into emission from S IV $\lambda\lambda$ 1062, 1072 and He II λ 1085.

As shown in the left panel of Figure 6, absorption is common at all luminosities, and over 50% (30 of 53) of the low-redshift Type 1 AGN observed using *FUSE* show detectable O VI absorption, comparable to those Seyferts that show longer-wavelength UV (Crenshaw et al. 1999) or X-ray (Reynolds 1997; George et al. 1998) absorption. None show intrinsic H₂ absorption. We see three basic morphologies for O VI absorption lines: (1) **Single**: 13 of 30 objects exhibit single, narrow, isolated O VI absorption lines, as illustrated by the spectrum of Ton S180 (Turner et al. 2001). PG0804+761, shown in the top panel of Figure 7, is another example. (2) **Blend**: multiple O VI absorption components that are blended together. 10 of 30 objects fall in this class, and the spectrum of Mrk 279 is typical (Scott et al. 2004). The middle panel of Figure 7 shows Mrk 478 as another example. (3) **Smooth**: The 7 objects here are an extreme expression of the “blend” class, where the O VI absorption is so broad and blended that individual O VI components cannot be identified. NGC 4151 typifies this class (Kriss et al. 1992, 1995; Kriss 2001). The mini-BAL QSO PG1411+442 is another example of this class, shown in the bottom panel of Figure 7.

Individual O VI absorption components in our spectra have FWHM of 50–750 km s^{−1}, with most objects having FWHM < 100 km s^{−1}. The multiple components that are typically present are almost always blue shifted, and they span a velocity range of 200–4000 km s^{−1}; half the objects span a range of < 1000 km s^{−1}. As shown in the right panel of Figure 6, the maximum outflow velocities show a tendency to increase with source luminosity, perhaps indicating

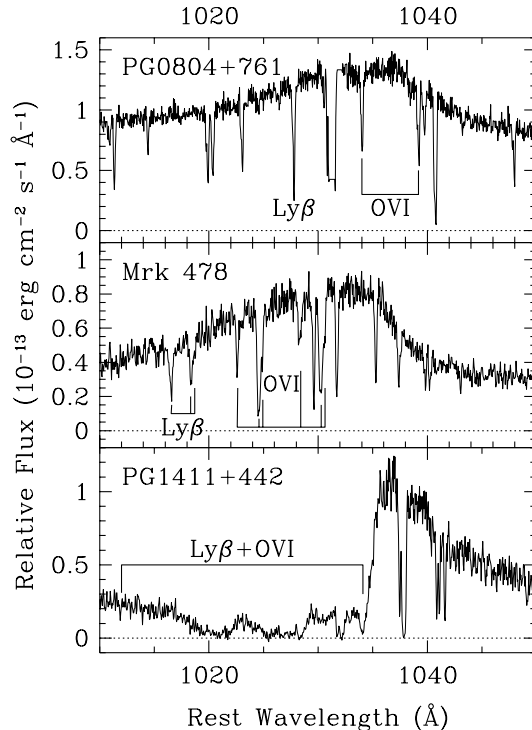


Figure 7. The three classes of O VI absorption line morphology: Single, isolated lines: PG0804+761 (top); Multiple, blended lines: Mrk 478 (middle); Broad, blended trough: PG1411+442 (bottom).

that radiative acceleration plays some role in the dynamics. Note also that there is a population of low-velocity absorbers present at all luminosities.

4. Mass Outflows from AGN

The absorption lines we see in our spectra of AGN are associated with mass outflows from the active nucleus. These outflows can profoundly affect the evolution of the central engine (Blandford & Begelman 1999), the host galaxy and its interstellar medium (Silk & Rees 1998; Wyithe & Loeb 2003) and also the surrounding intergalactic medium (IGM) (Cavaliere, Lapi, & Menci 2002; Granato et al. 2004; Scannapieco & Oh 2004). Winds from the high metal-abundance nuclear regions may be a significant source for enriching the IGM (Adelberger et al. 2003). Absorption by the outflow can also collimate the ionizing radiation (Kriss et al. 1997) and thereby influence the ionization structure of the host galaxy and the surrounding IGM.

The outflowing gas in AGN is sometimes visible as extended, bi-conical emission at visible or X-ray wavelengths (e.g., NGC 4151, Evans et al. 1993, Hutchings et al. 1998; NGC 1068, Ogle et al. 2003), but it most frequently manifests itself as blue-shifted absorption features in their UV and X-ray spectra. About half of all low-redshift AGN show X-ray absorption by highly ionized gas (Reynolds 1997; George et al. 1998), and a similar fraction show associated

UV absorption in ionized species such as C IV (Crenshaw et al. 1999) and O VI (Kriss 2001). In more luminous quasars, the fraction of objects in the Sloan Digital Sky Survey that shows broad C IV absorption troughs rises steeply as the troughs become narrower (Tolea, Krolik, & Tsvetanov 2002; Reichard et al. 2003), comprising over 30% of the quasar population at widths narrower than 1000 km s^{-1} . For AGN that have been observed in both the X-ray and the UV, there is a one-to-one correspondence between objects showing X-ray and UV absorption, implying that the phenomena are related in some way (Crenshaw et al. 1999). The high frequency of occurrence of UV and X-ray absorption suggests that the absorbing gas has a high covering fraction, and that it is present in all AGN. The gas has a total mass exceeding $\sim 10^3 M_{\odot}$ (greater than the broad-line region, or BLR), and is outflowing at a rate $> 0.1 M_{\odot} \text{ yr}^{-1}$ ($10\times$ the accretion rate in some objects) (Reynolds 1997). In an effort to understand AGN outflows better, *FUSE* guest investigators have been successful in coordinating several campaigns on bright AGN with simultaneous *HST* and X-ray observations of NGC 3783, NGC 5548, NGC 4051, NGC 4151, Ark 564, Mrk 279, and NGC 7469.

Some of the key results from these campaigns are:

- Doublet ratios for the O VI absorption lines show that the absorbers can be optically thick, but they are not black at line center. Thus column densities are frequently underestimated, sometimes by as much as an order of magnitude (Arav, Korista, & de Kool 2002; Arav et al. 2003).
- Variations in the absorption line strength can reflect either an ionization response, or bulk motion (Crenshaw et al. 1999; Gabel et al. 2003b).
- In the extensive recent *Chandra/FUSE/HST* campaign on NGC 3783 (Kaspi et al. 2002; Gabel et al. 2003a), the kinematics of the X-ray absorbing gas provide a good match to the UV-absorbing gas. The X-ray absorbing gas itself contains material spanning a large range of ionization parameters (Lee et al. 2002; Sako et al. 2003; Netzer et al. 2003), and it is likely that this broad range of physical conditions can also include the UV-absorbing ions. This is a natural prediction of the thermally driven wind model of Krolik & Kriss (1995, 2001), and would also be likely in disk-driven winds.
- In other cases the UV gas visible in *FUSE* spectra appears to be in a fairly low ionization state, and there is no direct relation between the X-ray absorption and the multiple kinematic components seen in the UV (NGC 5548: Brotherton et al. 2002; Mrk 509: Kriss et al. 2000; Yaqoob et al. 2003; NGC 7469: Kriss et al. 2003; Blustin et al. 2003).

The multiple kinematic components frequently seen in the UV absorption spectra of AGN clearly show that the absorbing medium is complex, with separate UV and X-ray dominant zones. In some cases, the UV absorption component corresponding to the X-ray warm absorber can be clearly identified, such as NGC 3783 (Kaspi et al. 2002; Gabel et al. 2003a; Netzer et al. 2003). In others, however, *no* UV absorption component shows physical conditions characteristic of those seen in the X-ray absorber as in NGC 5548 (Brotherton et al. 2002). One potential geometry for this complex absorbing structure is high-density, low-column UV-absorbing clouds embedded in a low-density, high-ionization medium that dominates the X-ray absorption.

Disk-driven winds are a possible explanation for some cases of AGN outflows (Königl & Kartje 1994; Murray et al. 1995; Elvis 2000; Proga 2000). By analogy to stellar winds, one would expect the terminal velocity of an AGN outflow to reflect the gravity of its origin. Disk-driven winds should therefore have velocities in the range of several thousand km s^{-1} . Objects with broad, smooth profiles might fall in this category. The geometry proposed by Elvis (2000) suggests that these objects should have only modest inclinations. However, two prime examples of Seyferts with broad smooth absorption troughs, NGC 3516 (Hutchings et al. 2001) and NGC 4151 (Kriss 2001), are likely the highest inclination sources in our sample given their extended, bi-conical narrow emission-line region morphologies (Miyaji, Wilson, & Perez-Fournon 1992; Evans et al. 1993) and their opaque Lyman limits (Kriss et al. 1997).

The lower velocities we observe in objects like NGC 3783 and NGC 5548 are more compatible with thermally driven winds from the obscuring torus (Krolik & Kriss 1995, 2001). In these thermally driven winds, photoionized evaporation in the presence of a copious mass source (the torus) locks the ratio of ionizing intensity to total gas pressure (the ionization parameter Ξ) at a critical value. For AGN spectral energy distributions lacking a strong extreme ultraviolet bump, such as the composite spectra of quasars assembled by Zheng et al. (1997), Laor et al. (1997), and Telfer et al. (2002), the ionization equilibrium curve exhibits an extensive vertical branch. Thus, at the critical ionization parameter for evaporation, there is a broad range of temperatures that can coexist in equilibrium at nearly constant pressure. For this reason, the flow is expected to be strongly inhomogeneous. Outflow velocities are typical of the sound speed in the heated gas, or several hundred km s^{-1} , comparable to the velocities seen in many AGN.

In summary, we find that O VI absorption is common in low-redshift ($z < 0.15$) AGN. 30 of 53 Type 1 AGN with $z < 0.15$ observed using *FUSE* show multiple, blended O VI absorption lines with typical widths of $\sim 100 \text{ km s}^{-1}$ that are blueshifted over a velocity range of $\sim 1000 \text{ km s}^{-1}$. Those galaxies in our sample with existing X-ray or longer wavelength UV observations also show C IV absorption and evidence of a soft X-ray warm absorber. In some cases, a UV absorption component has physical properties similar to the X-ray absorbing gas, but in others there is no clear physical correspondence between the UV and X-ray absorbing components.

Acknowledgments. I thank all the members of the *FUSE* AGN Working Group for their contributions to this research, especially Jennifer Scott and Zhaohui Shang. This work is based on data obtained for the Guaranteed Time Team by the NASA-CNES-CSA *FUSE* mission operated by the Johns Hopkins University. Financial support to U. S. participants has been provided by NASA contract NAS5-32985.

References

- Adelberger, K. L., et al. 2003, ApJ, 584, 45
- Arav, N., Korista, K. T., & de Kool, M. 2002, ApJ, 566, 699
- Arav, N., et al. 2003, ApJ, 590, 174
- Blandford, R. D., & Begelman, M. C. 1999, MNRAS, 303, L1
- Blustin, A., et al. 2003, *a*, 403, 481

- Brotherton, M., et al. 2002, *ApJ*, 565, 800
 Cavaliere, A., Lapi, A., Menci, N., 2002, *ApJ*, 581, L1
 Crenshaw, D. M., et al. 1999, *ApJ*, 516, 750
 Elvis, M. 2000, *ApJ*, 545, 63
 Evans, I., et al. 1993, *ApJ*, 417, 82
 Gabel, J., et al. 2003a, *ApJ*, 583, 178
 Gabel, J., et al. 2003b, *ApJ*, 595, 120
 George, I. M., et al. 1998, *ApJS*, 114, 73
 Granato, G. L., et al. 2004, *ApJ*, 600, 580
 Hubeny, I., Agol, E., Blaes, O., & Krolik, J. H. 2000 *ApJ*, 533, 710
 Hutchings, J., et al. 1998, *ApJ*, 492, L115
 Hutchings, J., et al. 2001, *ApJ*, 559, 173
 Kaspi, S., et al. 2002, *ApJ*, 574, 643
 Königl, A., & Kartje, J. F. 1994, *ApJ*, 434, 446
 Kriss, G. A. 2001, in *Mass Outflows in Active Galactic Nuclei: New Perspectives*, ed. D. M. Crenshaw, S. B. Kraemer, & I. M. George, A. S. P. Conference Series, 255, 69 (ASP: San Francisco)
 Kriss G. A., et al. 1992, *ApJ*, 392, 485
 Kriss G. A., et al. 1995, *ApJ*, 454, L7
 Kriss G. A., et al. 1997, in *proceedings IAU Colloquium 159*, ed. B. M. Peterson, F.-Z. Cheng, & A. S. Wilson, A. S. P. Conference Series, 113, 453 (ASP: San Francisco)
 Kriss, G. A., et al. 2000, *ApJ*, 538, L17
 Kriss, G. A., et al. 2003, *Å*, 403, 473
 Krolik, J. H., & Kriss, G. A. 1995, *ApJ*, 447, 512
 Krolik, J. H., & Kriss, G. A. 2001, *ApJ*, 561, 684
 Laor, A., et al. 1997, *ApJ*, 477, 93
 Lee, J. C., et al. 2002, in *X-ray Spectroscopy of AGN with Chandra and XMM-Newton*, ed. T. Böller (<http://www.xray.mpe.mpg.de/~bol/agnspec/programm.html>)
 Murray, N., et al. 1995, *ApJ*, 451, 498
 Miyaji, T., Wilson, A., & Perez-Fournon, I. 1992, *ApJ*, 385, 137
 Netzer, H., et al. 2003, *ApJ*, 599, 933
 Ogle, P., et al. 2003, *Å*, 402, 849
 Proga, D. 2000, *ApJ*, 538, 684
 Reichard, T. A., et al. 2003, *AJ*, 125, 1711
 Reynolds, C. S. 1997, *MNRAS*, 286, 513
 Sako, M., et al. 2003, *ApJ*, 596, 114
 Scannapieco, E. & Oh, S. P. 2004, *ApJ*, 608, 62
 Scott, J. E., et al. 2004, *ApJ*, 615, 135
 Shang, Z., et al. 2004, *ApJ* in press (astro-ph/0409697).
 Silk, J., & Rees, M. J. 1998, *Å*, 331, L1S.
 Telfer, R. C., et al. 2002, *ApJ*, 565, 773
 Tolea, A., Krolik, J. H., & Tsvetanov, Z. 2002, *ApJ*, 578, L31
 Turner, T. J., et al. 2001, *ApJ*, 548, L13
 Wyithe, J. S. B. & Loeb, A. 2003, *ApJ*, 595, 614
 Yaqoob, T., et al. 2003, *ApJ*, 582, 105
 Zheng, W., et al. 1997, *ApJ*, 475, 469